

Optical studies of metal doped As-prepared and Annealed Te-rich thin films $\text{Te}_{90}\text{Se}_{10}$ and $\text{Te}_{80}\text{Se}_{10}\text{M}_{10}$

Arvind Kumar Verma, Pramesh Chandra, Anchal Srivastava and R.K Shukla

Department of Physics, University of Lucknow, Lucknow – 226007, India

Corresponding Author: Arvind Kumar Verma

Abstract: This work is devoted to synthesising thermally evaporated as-prepared and annealed thin-film of high-quality nature from metal doped Te-rich $\text{Te}_{90}\text{Se}_{10}$ and $\text{Te}_{80}\text{Se}_{10}\text{M}_{10}$ ($M=\text{Cd}, \text{Hg}$). Glass substrates were used to deposit the film samples from input constituent elements, which have a purity degree 99.999%. XRD pattern of the thin film shows the formation of partially crystalline structure and a combination of amorphous and crystalline nature and crystallinity is changed by changing the metallic additives. Furthermore, the particle size and crystallinity of the film increases while the dislocation density decreases. FESEM image shows that morphology of the films is in a nanosize regime. Spectral dependence of optical absorption spectra in the wavelength range 200 – 2500 nm has been used to calculate the optical parameters of as-prepared and annealed thin-film at various compositional variations. Optical constants; absorption coefficient (α), optical band gap (E_g) and absorption constant are calculated at room temperature. Optical absorption is varied at various components (Cd, Hg) with increasing wavelength in NIR region. The optical band gap of both films as a function of photon energy. It has been found that the optical band gap varies in the present system. Luminescence of all films observed in the visible region (green colour) at 430 nm excitation wavelength.

Keywords: Thin films, XRD, FESEM, UV/VIS/NIR, PL.

Date of Submission: 05-07-2017

Date of acceptance: 10-08-2017

I. Introduction

The attention in this paper is focussed on discussing the optical properties of metal-doped chalcogenide as-prepared and annealed film on glass substrate because if any glass is free of defects such as bubbles or imperfections; it can be considered that a glass is a perfect material for optical studies[1]. Chalcogenide glasses are an oxygen-free inorganic glass containing one or more kinds of chalcogen elements (Te, Se)[2]. The increase of Te content leads to the formation of composition with a higher degree of disorder and hence higher densities of localised states. Chalcogenide glasses are generally less strong more weakly bonded materials than oxide glasses. The change in the optical properties of the composition may be explained by assuming that Te atoms act as an impurity centre in the mobility gap[3]. Te based glasses, due to their extreme tendency to crystallise the photosensitive chalcogenide thin films are promising candidates for a variety of applications such as information storage, photonics, optomechanical transducers, etc [4, 5]. Chalcogenide glasses are being studied mostly for applications as passive devices (lenses, windows, fibres) but these glasses are also attractive for the preparation of active devices such as laser fibre amplifiers and non-linear components [6].

It is well known that the addition of some metallic additives to binary chalcogenide glasses, changes their structure and new properties are expected for these glasses. From this point of view, the addition of metals (Cd, Hg) to the Te-Se binary system can be markedly affecting its optical properties. We have performed optical band gap (E_g), the absorption coefficient (α) and absorption constant by optical absorption and luminescence properties by PL for as-prepared and annealed $\text{Te}_{90}\text{Se}_{10}$ and $\text{Te}_{80}\text{Se}_{10}\text{M}_{10}$ ($M=\text{Cd}, \text{Hg}$) thin films to see the metal-induced effects on the optical properties for advanced application in future.

II. Experimental Procedure

In the present work, melt quenching method has been adopted to prepare $\text{Te}_{90}\text{Se}_{10}$ and $\text{Te}_{80}\text{Se}_{10}\text{M}_{10}$ ($M=\text{Cd}, \text{Hg}$) alloys. One of the most important features of melt quenching technique is the high flexibility of geometry and composition and the advantage of obtaining materials in desired quantities. Chalcogenide alloy $\text{Te}_{90}\text{Se}_{10}$ and $\text{Te}_{80}\text{Se}_{10}\text{M}_{10}$ ($M=\text{Cd}, \text{Hg}$) were prepared from 99.999% pure constitute elements (Te, Se, Cd, Hg). The exact amount of alloying elements were weighed according to their atomic weight percentages using an electronic balance with the least count of a 10^{-4} gram and then placing into ultra-cleaned quartz ampoules (length ≈ 5 cm and internal diameter ≈ 8 mm). The ampoules were evacuated and sealed under a vacuum of 10^{-3} torr with an oxygen-indane flame torch using rotary pumps to avoid reaction of alloying elements with oxygen at a higher temperature. The sealed ampoules were heated in a furnace at the rate of $4^{\circ}\text{C}/\text{min}$. The temperature was

raised up to $1000^{\circ}C$ and was maintained for 10 hours. During the heating process, the ampoules were constantly rocked by a ceramic rod to ensure the homogeneity of the alloying materials. After 10 hours the ampoules with molten materials were rapidly quenched into the ice-cooled water to allow glass formation and to avoid crystallisation. Quenching samples were removed from the ampoules by breaking the quartz ampoules. The material turned into a black solid which was recovered from the quartz ampoule and crushed into powder form and filtered to obtain homogeneous alloys. Obtained as-prepared sample is further annealed for 4 hours at $250^{\circ}C$ fixed temperature to remove internal stress to make the material less brittle and each sample is named as S1 ($Te_{90}Se_{10}$), S2 ($Te_{80}Se_{10}Cd_{10}$) and S3 ($Te_{80}Se_{10}Hg_{10}$). Using this as source material for thin films were deposited onto chemically cleaned glass substrates by thermal evaporation technique in a vacuum better than 10^{-4} bar using a Hind High Vacuum coating unit (model 12A4D). The thickness of the film S1, S2, and S3 are 221, 173 and 95 nm respectively measured by a single crystal thickness monitor. The amorphous/crystalline nature and crystal structure of the as-prepared and annealed thin-film of $Te_{90}Se_{10}$ and $Te_{80}Se_{10}M_{10}$ ($M=Cd, Hg$) were characterized by X-ray diffraction (XRD) using Ultima IV model from Rigaku, Japan employing $Cu K_{\alpha}$ radiation (wavelength 1.5404 \AA) in the 2θ range from 20° to 80° with scan speed of $2^{\circ}/sec$, Surface morphology by JSM-7610F Model FESEM from JEOL, Japan, A JASCO V-670, UV/VIS/NIR computerized spectrophotometer were used for measuring optical absorption of the both thin films measured as a function of wavelength and Photoluminescence (PL) spectra were recorded with LS55 Perkin Elmer Fluorescence spectrometer at 430 nm excitation wavelength .

III. Results And Discussion

3.1 X-RAY DIFFRACTION

The X-ray diffraction technique was employed for studying the structural details of the as-prepared and annealed thin-film of the $Te_{90}Se_{10}$ and $Te_{80}Se_{10}M_{10}$ ($M=Cd, Hg$) alloys, deposited on glass substrate. Figure 1, shows the X-ray diffraction traces of as-prepared and annealed thin-film. XRD pattern of the thin film sample S1, S2, and S3 shows the formation of partially crystalline structure and a combination of amorphous and crystalline nature. The individual crystallite size of all the films has been determined using the Scherer's formula as [7]. Crystallite size (D) = $K\lambda/\beta_s \cos\theta$, Where λ is the wavelength of the X-ray (1.5406 \AA), β is the width of a strong peak at half maximum intensity (FWHM) and θ is the corresponding Bragg diffraction angle and the Scherer constant (K) is of the order of unity. Using the crystallite size, the rough approximation of a number of defects in the film is defined by dislocation density (δ) have been calculated using the following formula [8]; $\delta = n/D^2$ Where n is a factor, which equals unity giving minimum dislocation density. The crystallite size D and dislocation density (δ) have been calculated using above formula and all values are given in Table 1. It is suggested that when the dislocation density is fairly high there is an increase in the band gap of the synthesised material because of the presence of dislocation that is separated by a distance greater than the inter-atomic distance [9].

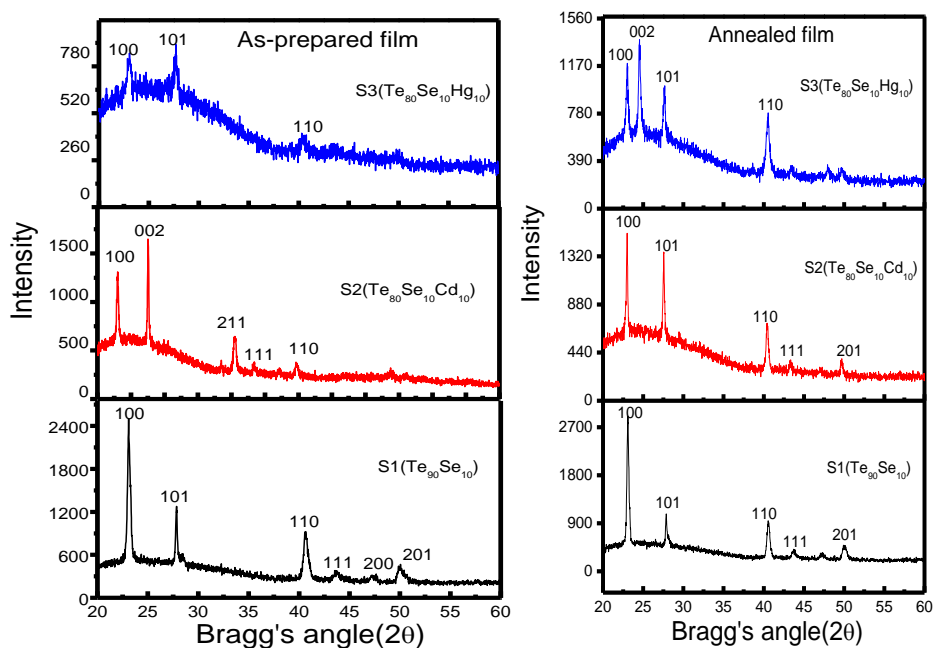


Fig.1: X-ray pattern of the as-prepared and annealed $Te_{90}Se_{10}$ and $Te_{80}Se_{10}M_{10}$ ($M=Cd, Hg$) thin films.

The peaks observed by as-prepared and annealed thin films of S1, S2 and S3 at 100, 201 confirm the hexagonal phase and the one observed at 101 confirm the cubic phase as concluded from DB card no. (000040554). Larger band gap and high amount of defects (higher dislocation density) in terms of localised state are responsible for increasing or decreasing the crystal size of the film sample.

3.2 SURFACE MORPHOLOGY

In FESEM, the electrons interact with atoms in the sample which produces various signals that can be detected. This gives important information regarding growth mechanism, shape, and size of the samples. Fig. 2 shows the Field Emission Scanning Electron Micrographs of the as-prepared and annealed film S1, S2 and S3 for $Te_{90}Se_{10}$ and $Te_{80}Se_{10}M_{10}$ ($M=Cd, Hg$); it can be observed that the surface morphology of the film has been changed with a dopant concentration of Cd and Hg. In the as-prepared film, undoped film S1 (Image-a) seems with a narrow distribution of grain sizes due to composed of close-packed nanoparticles, arrayed regularly on the substrate. Cd-doped film S2 (Image-b) is rough due to the irregular stacking of the grains on the substrate and Hg-doped film S3 (Image-c) observed some agglomerated grains and a porous structure with some cracks. This may be due to the formation of stresses by the difference in the ions size between doped content (Cd, Hg) with Te-Se system. Similarly, in thermally annealed film from Image-d for S1, the grain size decreases as compare to Image-a. In Image-e of the film, S2 shows grain size much clear as compare to Image-b and finally in Image-f for film S3, the grain size increases in compare to Image-c.

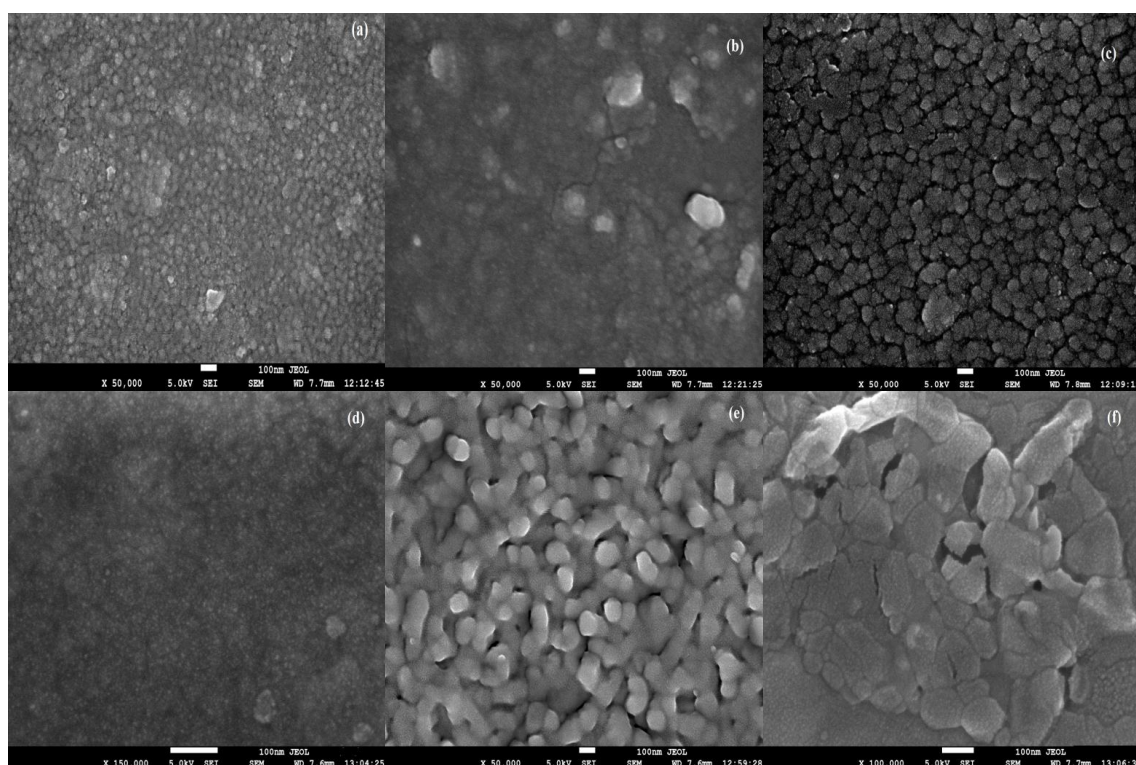


Fig.2: FESEM images of the as-prepared and annealed $Te_{90}Se_{10}$ and $Te_{80}Se_{10}M_{10}$ ($M=Cd, Hg$) thin films for S1, S2, S3.

Change in grain size of as-prepared and annealed films with changing dopant concentration as indicated by FESEM image which confirms the correctness of XRD data. From FESEM images most of the grain size observed between 20 to 60 nm ranges.

| Composition | Average crystallite Size (nm) | | Average dislocation density (nm^{-2}) | |
|-------------------------------|-------------------------------|----------|---|----------|
| | As-prepared | Annealed | As-prepared | Annealed |
| S1($Te_{90}Se_{10}$) | 20.44 | 25.92 | 0.002394 | 0.001488 |
| S2($Te_{80}Se_{10}Cd_{10}$) | 26.76 | 40.7 | 0.001396 | 0.000604 |
| S3($Te_{80}Se_{10}Hg_{10}$) | 4.2 | 27.92 | 0.056689 | 0.001283 |

3.3 OPTICAL ANALYSIS

The most interesting optical processes of the optical analysis in thin films are the absorption and emission of light. Basically, incident photons having energies greater than the optical band gap of the materials are absorbed and photons of incident light having energies less than the bandgap are transmitted through the materials. Absorption of an incident photon light of suitable frequency by the thin films permits a determination of the optical band gap of the synthesised materials that generates charge carriers are depending on properties of the material, the thickness of the films and wavelength of the incident photons [10]. The optical energy gap and the type of optical transition responsible for optical absorption, direct or indirect [11]. The optical band gap of the film under investigation has been calculated from the knowledge of the absorption data obtained from UV/VIS/NIR spectrophotometer. This part includes the results of absorption measurements, and their relation to wavelength. From these measurements, optical constants like absorption coefficient, optical band gap, and absorption constant were calculated.

3.3.1 ABSORPTION MEASUREMENTS

The optical absorption spectra of the as-prepared and annealed $Te_{90}Se_{10}$ and $Te_{80}Se_{10}M_{10}$ ($M=Cd, Hg$) thin film as a function of wavelength in the range (200- 2500 nm) as shown in Figure 3. In the as-prepared film, the optical absorption of the undoped film S1 observed at 879 nm in NIR region whereas, in doped film S2 (Cd-doped) and S3 (Hg-doped) observed at 269 and 244 nm in near ultraviolet region and gradually decreases with increasing wavelength. Similarly, in thermally annealed film optical absorption observed at 963 nm in undoped film S1 whereas in doped film S2 and S3 absorption observed between near ultraviolet and NIR region at 278,862 nm and 281,859 nm respectively.

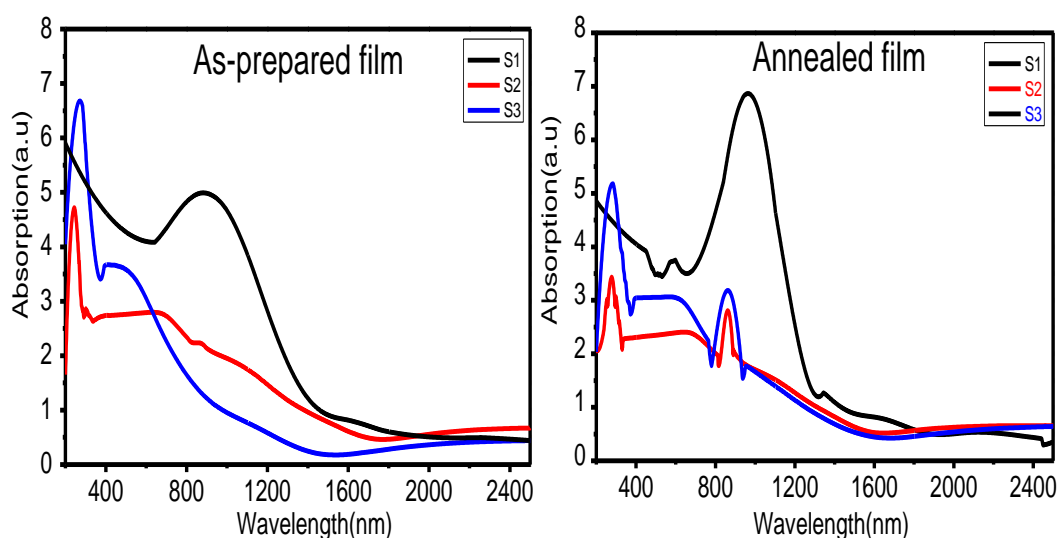


Fig.3: Optical absorption of the as-prepared and annealed $Te_{90}Se_{10}$ and $Te_{80}Se_{10}M_{10}$ ($M=Cd, Hg$) thin films.

3.3.2 ABSORPTION COEFFICIENT

Absorption coefficient (α) is the property of a material which defines the amount of light absorbed by it and depends upon photons energy as well as the nature of the material. Variation of absorption coefficient (α) with photon energy can be explained in term of fundamental absorption, excitation absorption and valence band acceptor absorption [12]. For many glasses and amorphous non-metallic materials, the absorption edge can be divided into three distinct regions; (i) high absorption region ($\alpha \geq 10^4 \text{ cm}^{-1}$) where absorption is associated with inter-band transitions involving optical transitions between valence band and conduction band which determines the optical band gap, (ii) Spectral region with α in the range of $10^2 - 10^4 \text{ cm}^{-1}$ is called Urbach's exponential tail region in which absorption depends exponentially on photon energy. In this region, most of the optical transitions take place between localized states and extended band states which provides information about the relative changes of the structural disorder induced by an additive [13], (iii) low absorption region ($\alpha < 1 \text{ cm}^{-1}$) implies weak absorption tail involving low energy absorption and originates from defects and impurities whose shape and magnitude depends on the purity, thermal history and preparation conditions [14, 15].

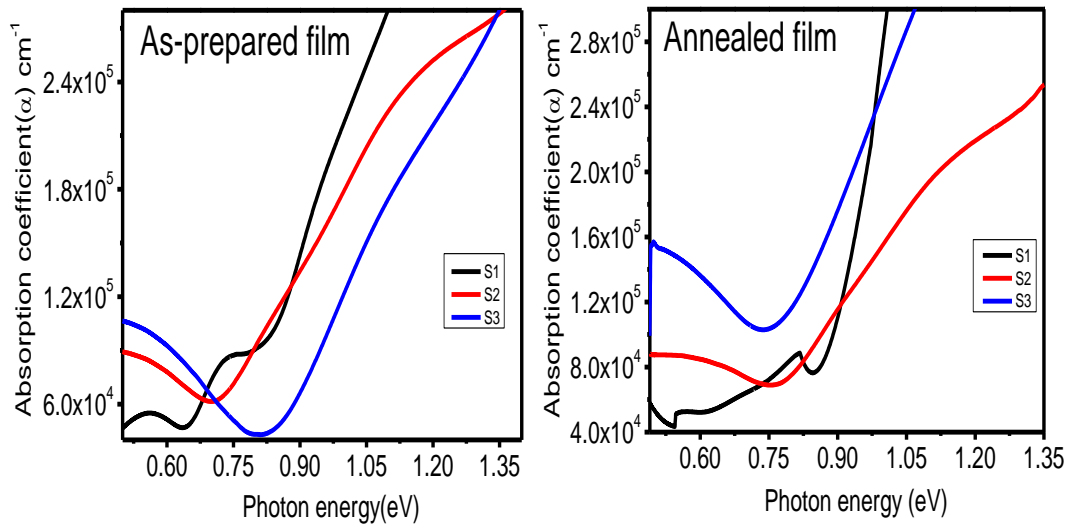


Fig. 4: Absorption coefficient with photon energy for as-prepared and annealed $Te_{90}Se_{10}$ and $Te_{80}Se_{10}M_{10}$ ($M=Cd, Hg$) thin films.

The absorption coefficient (α) has been evaluated by Beer-Lambert law ($\alpha=2.303*A/t$), Where A is optical absorption which depends on wavelength and density of point defects and (t) is the thickness of the films [23]. Figure 4 shows the absorption coefficient of the as-prepared and annealed film; S1, S2, S3 for $Te_{90}Se_{10}$ and $Te_{80}Se_{10}M_{10}$ ($M=Cd, Hg$) with incident photon energy range. The absorption coefficient observed in high absorption region for all thin films, not in the weak absorption region which is associated with inter-band transitions. The absorption coefficient (α) has been observed to change with an increase in photon energy as well as change with metal additive composition. The absorption coefficient of the as-prepared film S1 has maximum value with respect to Cd-doped film S2 and Hg-doped film S3 respectively. In the same manner in thermally annealed film absorption coefficient of the film, S3 has maximum value against S1, S2 at 0.74 eV. All the values of absorption coefficient for $Te_{90}Se_{10}$ and $Te_{80}Se_{10}M_{10}$ ($M=Cd, Hg$) thin films are given in Table 2.

3.3.3 OPTICAL BAND GAP

The energy at which electron and holes pair is generated is called optical band gap energy. The high absorption region determines the optical band gap energy. The optical energy gap was obtained from a plot of $(\alpha hv)^{1/2}$ vs hv , where α is absorption coefficient, h is plank's constant and ν is incident photon frequency. Figure 5 Shows the optical band gap of as-prepared and annealed $Te_{90}Se_{10}$ and $Te_{80}Se_{10}M_{10}$ ($M=Cd, Hg$) films by the direct transition because direct bandgap gives more favourable optoelectronic properties than the indirect bandgap [16]. The Expected value of optical band gap for as-prepared and annealed film S1, S2 and S3 are given in Table 2. There are several reasons to determine the increase or decrease the optical band gap of the chalcogenide thin films. Reduction in the value of measured optical band gap for as-prepared and annealed film with respect to undoped film S1 due to increment of charged defects in the band tail regions, which leads to reducing the optical band gap [17] or the reduction in the optical gap can be explained according to Hese-gawa et al suggestion [18, 19]; according to them, the unsaturated bonds are responsible for the formation of localized tail states in the band gap. The presence of a high majority of these localised states is responsible for decreasing the optical band gap and this transformation is accompanied by an increase in crystallite size as evidenced by XRD pattern [20]. The addition of Te in the glass structure causes deeper band tails extended in the gap and thereby leading to a decrease in the value of optical band gap. The decrease of optical band gap with increasing Te content may also be related to the increasing number of bonds. Further, the optical band gap is strongly dependent on the fractional concentration of Te atoms because Te atoms to form chemical disordering and to create localised states in the forbidden gap [21] leading to lower the optical band gap.

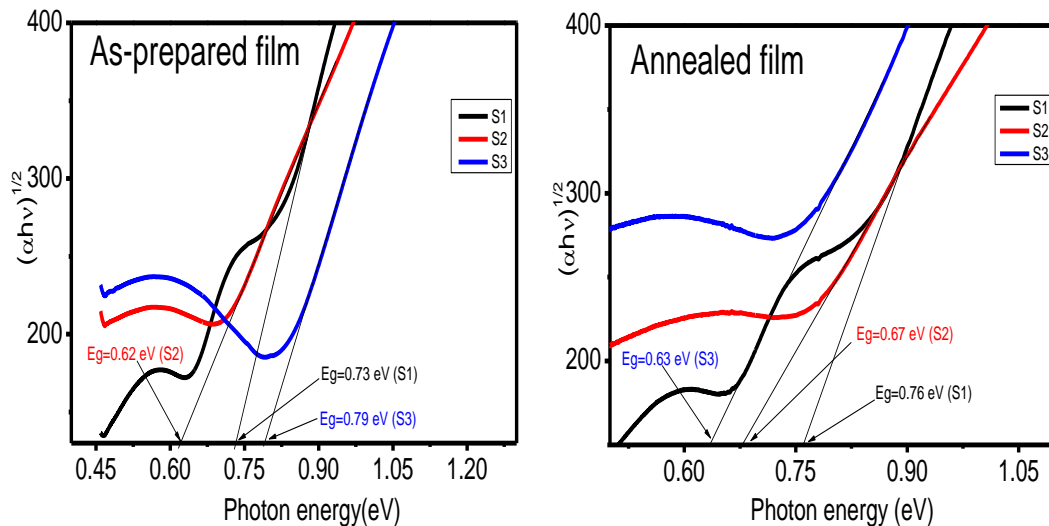


Fig.5: The photon energy dependence of optical band gap for as-prepared and annealed $Te_{90}Se_{10}$ and $Te_{80}Se_{10}M_{10}$ ($M=Cd, Hg$) thin films.

The increase of Te content leads to the formation of composition with a higher degree of disorder and hence higher densities of localised states [22,23]. Similarly, the increase in the optical band gap of Hg-doped film S3 of the as-prepared film as compared to S1 (undoped) due to the reduction in the disorder and decrease in density of defect states. This increment in the optical band gap can be correlated with Davis and Mott suggestion [24].

| Composition | Optical absorption in arb.unit | | Absorption coefficient(α) in $10^4 cm^{-1}$ at 0.74 eV | | Direct Optical band gap(E_g) In (eV) | | Absorption constant (K) | | Photoluminescence (nm) | |
|-------------------------------|--------------------------------|-------------------------|---|----------|--|----------|-------------------------|--------------------|------------------------|----------|
| | As-prepared | Annealed | As-prepared | Annealed | As-prepared | Annealed | As-prepared in 10^2 | Annealed in 10^8 | As-prepared | Annealed |
| S1($Te_{90}Se_{10}$) | 5.01 at 879 nm | 6.89 at 963 nm | 8.73 | 7.22 | 0.73 | 0.76 | 5.40 at 943 nm | 6.02 at 983 nm | 530,568 | 529,567 |
| S2($Te_{80}Se_{10}Cd_{10}$) | 6.70 at 269 nm | 3.47,2.82 at 278,862 nm | 6.95 | 6.87 | 0.62 | 0.67 | 2.09 at 720 nm | 2.49 at 864 nm | 532,570 | 530,567 |
| S3($Te_{80}Se_{10}Hg_{10}$) | 4.72 at 244 nm | 5.18,3.22 at 281,859 nm | 5.10 | 10.3 | 0.79 | 0.63 | 3.64 at 555 nm | 6.84 at 860 nm | 530,567 | 530,567 |

3.3.4 ABSORPTION CONSTANT

Absorption constant/Extinction coefficient indicates the amount of absorption loss when electromagnetic wave propagates through the films. The variations of absorption constant can be related to the variation of optical transmittance. Figure 6 shows the absorption constant of the as-prepared and annealed $Te_{90}Se_{10}$ and $Te_{80}Se_{10}M_{10}$ ($M=Cd, Hg$) thin film for S1, S2, S3 with increasing wavelength. The decrease in the absorption constant with increasing wavelength shows that the transmittance is increased. This behaviour is due to decrease in absorption coefficient with increasing wavelength of the incident photons. In as-prepared film; undoped film S1 has absorption loss in NIR region at 943 nm while in Cd-doped film S2 and Hg-doped film S3 shows minimum absorption loss in the visible region at 720, 555 nm respectively in the order of 10^2 ranges. Similarly in the thermally annealed film; Hg-doped film S3 has maximum absorption loss at 860 nm, as compare to undoped S1 and Cd-doped film S2 in NIR region at 10^8 order ranges and gradually increases as wavelength increases.

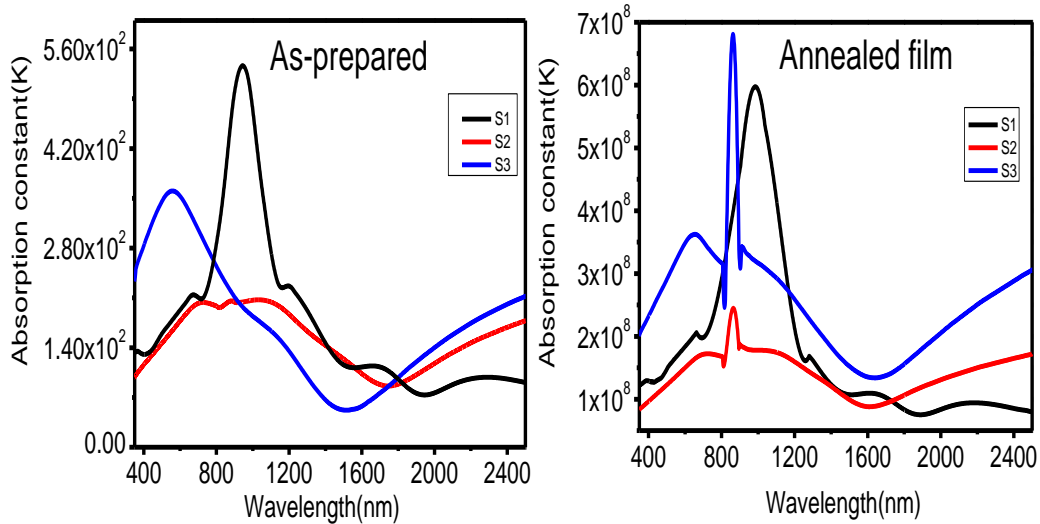


Fig. 6: Absorption constant with wavelength for as-prepared and annealed $Te_{90}Se_{10}$ and $Te_{80}Se_{10}M_{10}$ ($M=Cd, Hg$) thin films.

Rise and fall of absorption constant in the forbidden gap region are directly related to the absorption of light, the thickness of the film and nature of the materials. The absorption constant has been evaluated using formula $K=\lambda\alpha/4\pi$ [25, 26].

IV. Photoluminescence Spectroscopy

When charge carriers of the material are excited by the absorption of incident photons of suitable frequency, the resulting radiation (light emission) due to the recombination of excited charge carriers of electron and hole is known as photoluminescence and the property of light emission by the material is called luminescence.

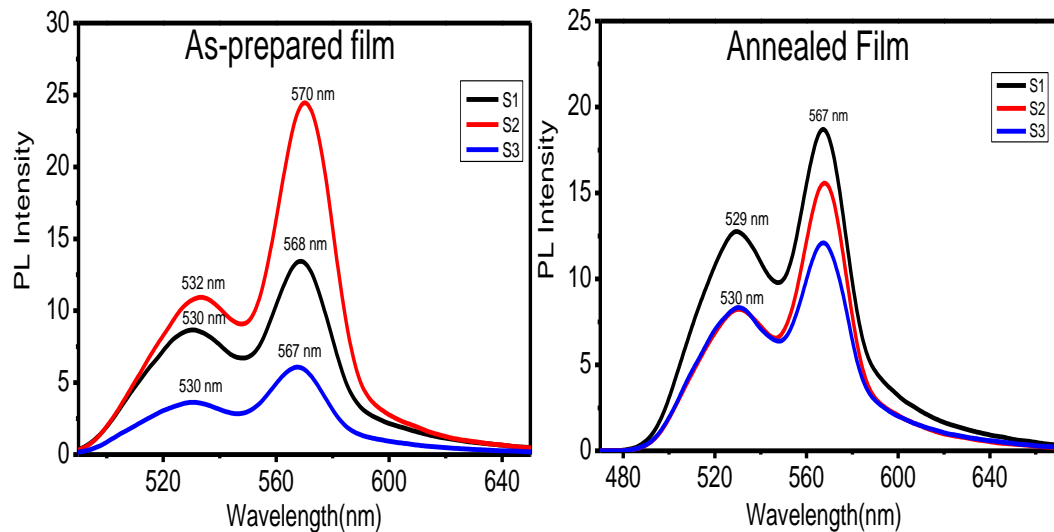


Fig. 7: Variation of PL intensity with wavelength for as-prepared and annealed $Te_{90}Se_{10}$ and $Te_{80}Se_{10}M_{10}$ ($M=Cd, Hg$) thin films.

Photoluminescence spectra were recorded using excitation wavelength at 430 nm for as-prepared and annealed $Te_{90}Se_{10}$ and $Te_{80}Se_{10}M_{10}$ ($M=Cd, Hg$) films in figure 7. Light emission for as-prepared and annealed film S1, S2, S3 is found to be centred around two wavelengths i.e. (530-532) and (567-570) nm due to the involvement of some oxygen vacancy concentration which increases the defects in the surface of the film resulting lowering the PL intensity in the visible region. Observed photoluminescence of Cd-doped film S2 of the as-prepared film has maximum value than S1, S3 whereas in the thermally annealed film; undoped film S1 has maximum value in comparison to S2, S3 respectively [27].

V. Conclusions

In summary, we have successfully synthesised Te-rich as-prepared and annealed Te₉₀Se₁₀ and Te₈₀Se₁₀M₁₀ (M=Cd, Hg) thin films using thermal evaporation technique. Partially polycrystalline nature with the hexagonal and cubic phase of thin films was confirmed by XRD. FESEM image shows that morphology of the films is in a nanosize regime with an irregular shape. Optical parameters were investigated with the aids of the absorbance spectra of the thin films with increasing wavelength. The absorption coefficient of as-prepared and annealed films S1, S2, S3 has been observed in high absorption region associating with the interband transition and Hg-doped annealed film S3 has maximum absorption coefficient. Direct optical band gap values have been determined by Tauc's relation and the values of the optical band gap have found to vary as a number of composition changes in TeSe matrix. Absorption constant of the Cd-doped film S2 of the as-prepared film has a minimum loss in the visible region at 10² ranges and in the thermally annealed film; Hg-doped film S3 has a maximum loss at 10⁸ order range in NIR region. Luminescence of the both films observed in the visible region between 529-570 nm due to oxygen vacancy concentration in the Te-rich films. In our conclusion due to higher absorption coefficient by different metal doped at fixed percentage amount in Te-rich thin film S3 of annealed film, it may be used as optical memory devices as per scientific requirements.

Acknowledgement

Financial assistance from UGC New Delhi India vide project F.No 42-773/2013(SR) is gratefully acknowledged. Authors are thankful to U.P State Government for providing XRD facility through Centre of Excellence Scheme at the Department of Physics, University of Lucknow.

References

- [1] B. Bruno, C.B.pledel, and P.Lucas *Forming Glasses from Se and Te, Molecules* 14, 2009, 4337-4350.
- [2] V. Pandey and S.K.Tripathi, *Optical Properties of Amorphous Se_{100-x}Sb_x Thin Films, J. of Ovonic Research* 2, 2006, 67-76.
- [3] P.Sharma and S.C Katyal, *Optical study of Ge₁₀Se_{90-x}Te_x glassy semiconductors, Thin Solid Films. 515,2007,7966-7970.*
- [4] Feinleib, J. DeNeufville, J.Moss and S.C. Ovshinsky, *Appl. Phys. Lett* 18, 1971,254.
- [5] P. Krecmer, A. M. Moulin, R. J. Stephenson, T. Rayment, M. E. Well and S. R. Elliot, *Reversible Nanocontraction and Dilatation in a Solid Induced by Polarized Light, Science*, 277,1997,1799-802.
- [6] D.Lezal, J. Pedlikova, and J. Zavadila, *Chalcogenide Glasses for Optical and Photonics applications. Of Optoelectronics and Advanced Materials* 6, 2004, 133-137.
- [7] S. Subramanian and D. P. Padiyan, *Mate. Chem. Phys.* 107, 2008,392.
- [8] N.Tohge, T.Minami, and M.Tanaka. *J. Non-Cryst. Solid* 59, 1983,999.
- [9] R.Sathyamoorthy, and J. Dheepa, *J. Phys. Chem. Solids* 68, 2007,111.
- [10] J.Pankove and J. I, *Optical process in semiconducting thin films, Thin Solid Films, 90, 1982, 172.*
- [11] J. Tauc, R. Grigorovici, and A. Vancu, *Phy. Sta. Solidi.* 15,1966,627.
- [12] A.A. Al-Ghamdi, *Vacuum* 80, 2006, 400-405.
- [13] M.K.Halimah and A.S.Zainal, *Optical properties of ternary tellurite glasses, Materials Science-Poland.* 28,2010.
- [14] P. Petkov, M. Wuttig, P. Ilchev, and T. Petkova, *J. Opt. Adv. Materials* 5, 2003, 1101.
- [15] M. Devika, N.K. Reddy, K. Ramesh, H.R. Sumana, K.R.Gunasekhar, E.S.R. Gopal, and K.T. Ramakrishna Reddy, *Semicond. Sci.Technol* 21, 2006, 1495.
- [16] M.C. Teich and BEA.Saleh, *Fundamentals of Photonics*, 1st edition. New York, Wiley, 1991.
- [17] K. Shimakawa, A. Kondo, K. Hayashi, S. Akahori, T. Kato, and S. R. Elliot, *Photoinduced metastable defects in amorphous semiconductors: communnality between hydrogenated amorphous silicon and chalcogenides, J.Non-Cryst. Solids* 387, 1993,164-166.
- [18] S.Hasegawa and S.Yazaki, *Solid State Commun.* 23, 1977, 41.
- [19] S.Hasegawa and M.Kitagawa, *Solis State Commun.* 27, 1978, 855.
- [20] S. Choudhary and S. K. Biswas, *J. Non-Cryst Solids*, 54, 1983,179.
- [21] N.F. Mott and E.A. Davis, *Electronic Processes in Non-Crystalline Materials*, Clarendon Press, Oxford, 1979.
- [22] P. Sharma, M. Vashistha and I.P. Jain, *J. Opt. Adv. Mater.* 7, 2005, 2647.
- [23] A. Ashour, N. El-Kdry, and S.A. Mahmoud, *Thin Solid Films* 269, 1995, 117.
- [24] N. Mott and E.A. Davis, *Electronic Processes in Non-crystalline Materials*, Clarendon Press, 1970.
- [25] A.A.Mulama1, J. M. Mwabora, A. O. Oduor, and C.C. Muiva, *Optical Properties and Raman Studies of Amorphous Se-Bi Thin Films, The African Review of Physics.* 9, 2014, 33.
- [26] V.Pandey, S.K.Tripathi and A.Kumar, *J. Optoelectronics and Advanced Materials* 8, 2006, 789-793.
- [27] D.Li, Y.H.Leung, A.B.Djurisic, Z.T.Liu, M.H.Xie, S.L.Shi, S.J.Xu and W.K.Chan, *Appl.Phys.Lett.*85, 2004, 1601.

IOSR Journal of Applied Physics (IOSR-JAP) is UGC approved Journal with Sl. No. 5010, Journal no. 49054.

Arvind Kumar Verma. "Optical studies of metal doped As-Prepared and Annealed Te-Rich thin films Te₉₀Se₁₀ and Te₈₀Se₁₀M₁₀." IOSR Journal of Applied Physics (IOSR-JAP), vol. 9, no. 4, 2017, pp. 67–74.